Author(s): S. Birkmann
Date of Issue: December 20, 2011
Version: 1

NIRSpec best focus positions during cycle 1 FM testing

Abstract:

This report describes the data, method, and results for estimating the best focus position of the NIR-Spec instrument, obtained during the first ground calibration campaign in February 2011. Given the analysis presented here, it is likely that NIRSpec will meet its focus related performance requirements.

1   INTRODUCTION

The NIRSpec instrument features a Re-focus Mechanism Assembly (RMA) as part of its fore optics. This unit determines the exact position where the focal surface of the JWST telescope (optical telescope element, OTE) is re-imaged onto the Micro-Shutter Assembly (MSA) plane. Therefore, the RMA must be able to compensate for any change in the OTE focal position that may occur during the JWST mission. Furthermore, the best focus for NIRSpec must be the same for all seven filters in the Filter Wheel Assembly (FWA), and also independent of the used apertures: MSA, fixed slits, or the Integral Field Unit (IFU).

2   SCOPE

The scope of this document is to present the analysis done of focus sweep data obtained during the first cycle of the NIRSpec FM instrument level tests, and to demonstrate that NIR-Spec will meet its focus related requirements given in the NIRSpec Functional Requirements Document (FRD, Smith 2008). The list of applicable requirements from the FRD is given in Append A.

3   THE DATA AND METHOD

All data presented here were taken during the first cryo cycle of the NIRSpec FM calibration campaign early 2011, mostly during the so-called "cold" phase with the NIRSpec bench
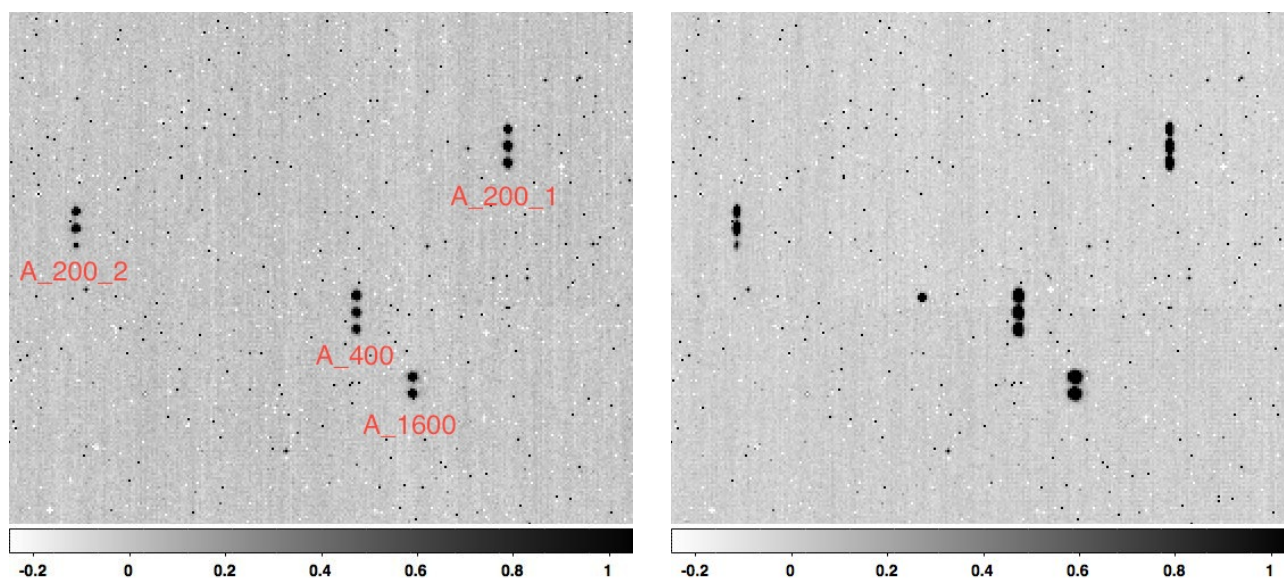
Figure 1: View of the pinhole images in the fixed slits, taken close to best focus (left) and when defocused by about 1.5 mm with the RMA. The bar at the bottom denotes the count rate in ADU/s. The elongated shape of the pinholes in the A_200 slits is clearly visible. Single dark pixels are due to high dark current in these pixels.

temperature set to $T_{\mathrm{bench}} = 31\,\mathrm{K}$. The names of the test sequences and the NIDs of the exposures obtained that are of relevance for this report are listed in Appendix B. Please see Ferruit (2011) for a complete overview of the cycle 1 test campaign. The data has been pre-processed using the NIRSpec pre-processing pipeline (Birkmann 2011b) to obtain count rate and uncertainty images and data quality maps. These products are then used with the IDL procedure sb_derive_focus.pro in the NIRSpec CVS repository to obtain the focus curves and derive the best focus for a given setting. The procedure fits two-dimensional Gaussians to the pinhole images and determines the full width at half maximum (FWHM).

During cycle 1 the MSA was not operational, therefore only point source images through the fixed slits and the IFU could be obtained. Since the 200 mas wide slits significantly clip the PSF even for moderate amounts of de-focus (see Fig. 1), the curves presented here were obtained using solely sources located in the A_400 and A_1600 slits. When using the pinhole mask, this corresponded to a total of 5 pinholes while in the case of the RCSS, the single point source was centered in the A1600 slit.

For the IFU, we obtained the focus curves from eight of nine pinholes located inside the $3{\times}3\,\mathrm{arcsec}^2$ IFU field of view. The pinholes were directly measured on the full detector frame, not on the reconstructed IFU image, selecting the most appropriate slitlet.

Focus sweeps were done with the pinhole mask (PHM) on the cryo mechanism (CMO) in place and also with the radiometric calibration spectral source (RCSS). Please see Birkmann (2011a) for a more comprehensive description of the NIRSpec OGSE. For the RCSS, there were five exposures per RMA position with the point source dithered inside the A_1600 slit to improve the sampling.

In the focus curves shown in this report, for each RMA position the point shown is the mean FWHM of the five pinholes measured (or the five measurements of the dithered RCSS exposures), and the error bar shown corresponds to the standard deviation of these individual FWHM measurements.

4 RESULTS

4.1 Focus sweeps for different CMO positions

At the beginning of the campaign, an initial focus sweep around the central RMA position was carried out using the test sequence PREP-FOCUS with the CMO in its nominal position ($z = 0$ mm). Preliminary analysis yielded a best focus value of approximately $-280\,\mu$m, and this value was used for the rest of the campaign when imaging pinholes with the CMO in its nominal z-position. Given the shallowness of the focus curves around best focus, deviations of $\sim \pm 100\,\mu$m seem to be acceptable without a significant broadening of the PSF.

This focus sweep was later repeated with the CMO at its nominal ($z = 0$ mm) and most extreme inward ($z = +2$ mm) and outward ($z = -3.1$ mm) z-position in the test sequence IMA-FOCUS using appropriate RMA centers for the curves. The results are shown in Fig. 2. From this we conclude that the best focus RMA position for the nominal CMO position is $\approx -330\,\mu$m for the pinholes in the fixed slits, close enough to the $-280\,\mu$m used during testing.

The IFU data yield a best focus value that is offset by approximately $+60\,\mu$m compared to the fixed slits for the three CMO z-positions tested.

The best focus position versus the CMO z-position follows a linear relationship (see Fig. 3), as is expected. A change Δz in CMO z-position can be compensated by an RMA movement of

$$\Delta\mathrm{RMA} = \frac{m^2}{\sqrt{2}}\Delta z, \tag{1}$$

where $m = f_{\mathrm{OTE}}/f_{\mathrm{MSA}}$ is the (de-)magnification from OTE to MSA plane ($f_{\mathrm{OTE}} \approx 20$, $f_{\mathrm{MSA}} \approx 12.5$). The $\sqrt{2}$ factor enters due to the penta-prism design of the RMA. Since we know the slope $\Delta\mathrm{RMA}/\Delta z = 0.2609 \pm 0.0027$ from Fig. 3 (for the pinholes in the fixed slits), we can compute the as-built magnification of the NIRSpec fore optics:

$$m = \sqrt{\sqrt{2}\frac{\Delta\mathrm{RMA}}{\Delta z}} = 0.6074 \pm 0.0031, \tag{2}$$

which nicely matches the values found for the NIRSpec DM (see e.g. The NIRSpec SOT 2008).

4.2 Filter confocality

One of the requirements in the FRD is that the best focus of NIRSpec should be independent of the filter used. This was tested with the test sequence PREP-CONFOCALITY-CHK, where the RMA was set to eleven position between -500 and $+500\,\mu$m in $100\,\mu$m steps and pinhole
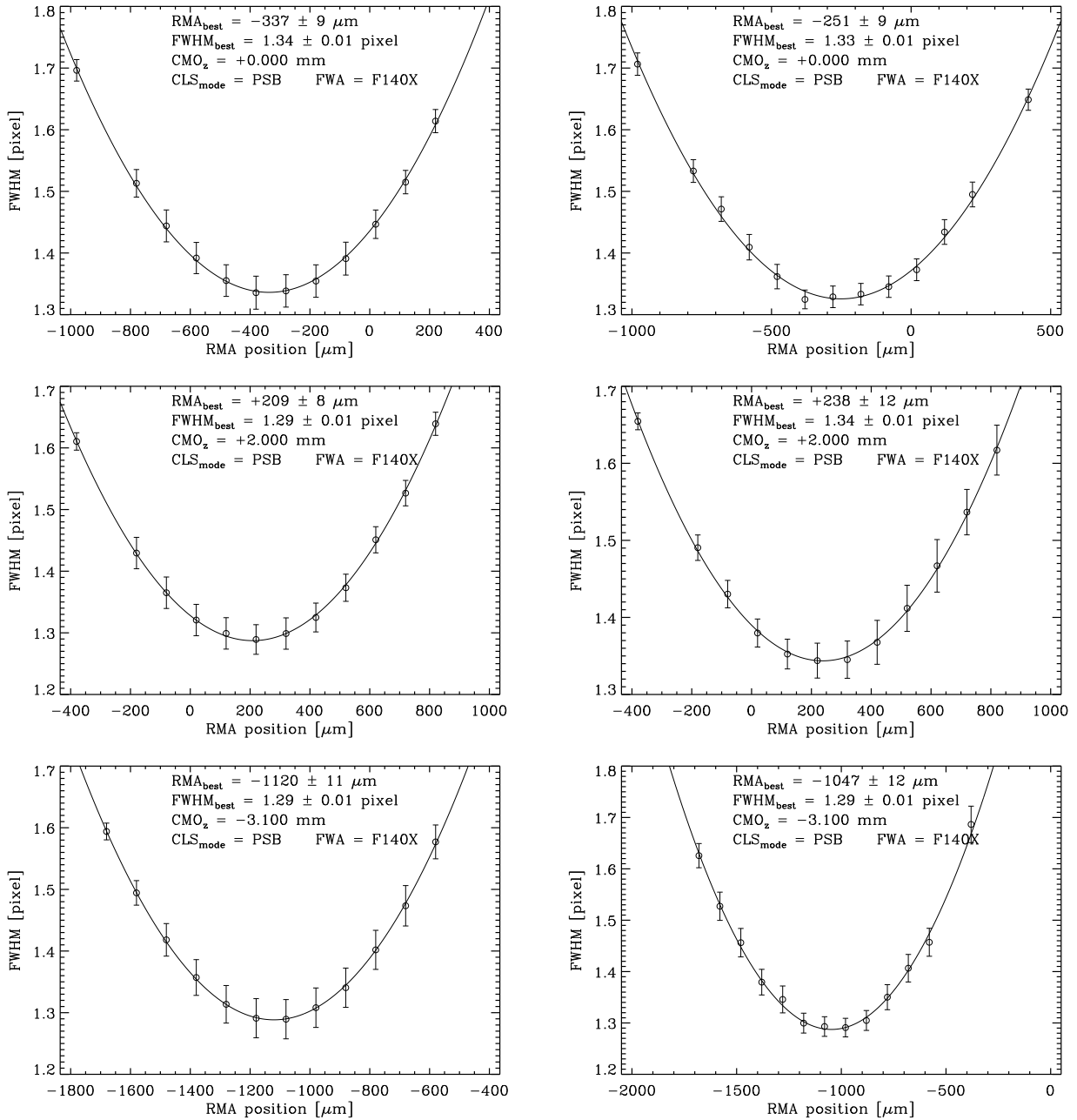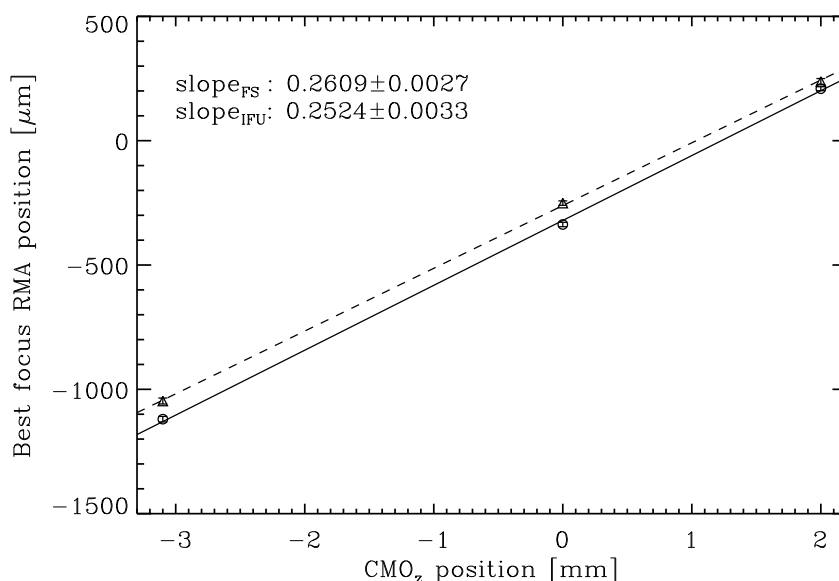
Figure 2: RMA focus sweeps taken with the IMA_FOCUS test sequence for the fixed slits (left column) and the IFU (right column) for three difference CMO z-positions.

Figure 3: Best focus RMA position versus CMO z-position for the fixed slits (circle symbols, solid line) and the IFU (triangles, dashed line).

images were obtained for each of the seven filters in the FWA. Because the best focus was actually for an RMA position around $-330\,\mu$m, this yielded focus curves with only a limited number of points on one side of the curve (see Fig. 4), leading to a higher uncertainty when determining the best focus for each filter from this data.

Judging from the available data, all filters show the same best focus position within the uncertainties, as is also evident from Fig. 5.

4.3 RCSS focus sweep

The result of the focus sweep with the RCSS is shown in Fig. 6. The best focus position ($\approx -630\,\mu$m) is offset by approximately $-300\,\mu$m compared to the one obtained with the PHM, suggesting that the alignment of the RCSS on the CMO in the z-position is off by $\approx -0.7\,$mm (away from NIRSpec). This is not a major issue and all subsequent RCSS related activities were carried out with the RCCS close to its best focus with the RMA set to $-700\,\mu$m. However, one should take care to combine RCSS calibration activities in cycle 2 in blocks to avoid frequent RMA movements.

It has to be noted that both plots in Fig. 6 were created using the same exposures. The only difference is that for the left panel, all 88 groups of the exposures were used, whereas for the right panel only the first 22 groups were taken into account. The latter approach yields smaller FWHM values for the RCSS, probably due to charge diffusion that sets in when a pixel accumulates more and more charge. A more detailed description of this effect is given by Sirianni & the SOT (2011).
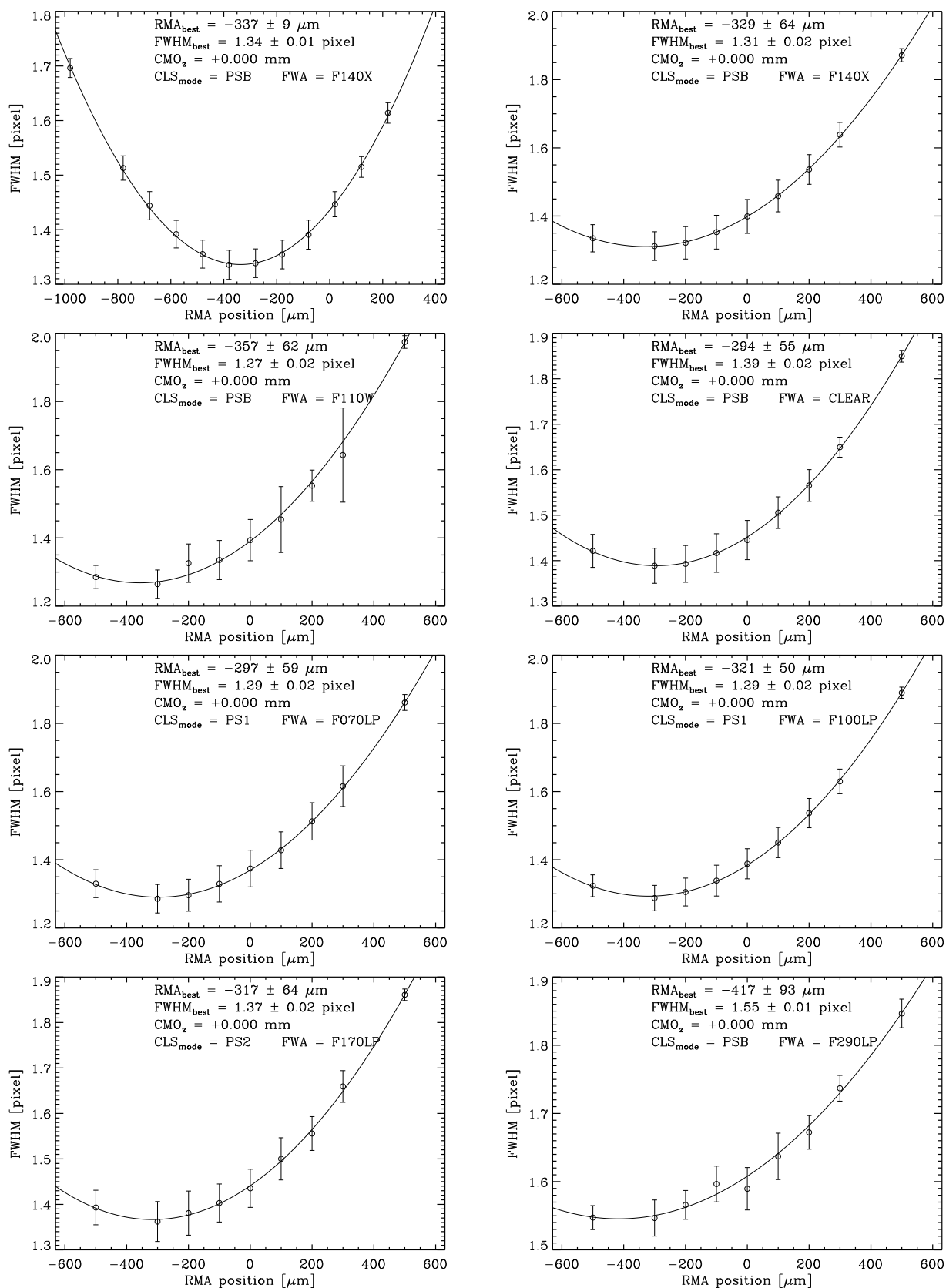
Figure 4: Focus curves for all NIRSpec filters. The top left curve is shown as reference.
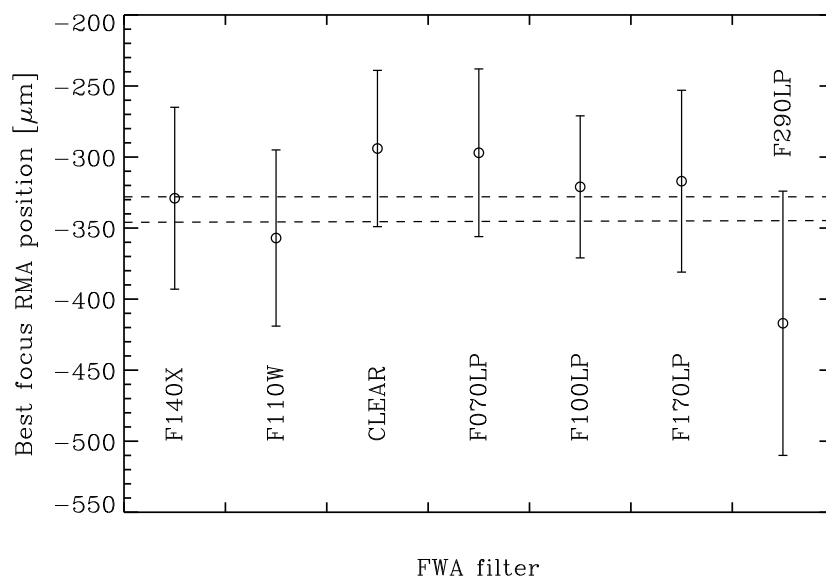
Figure 5: Best focus position for the NIRSpec filters. The dashed lines give the range of best focus determined with a full focus sweep in the F140X filter.
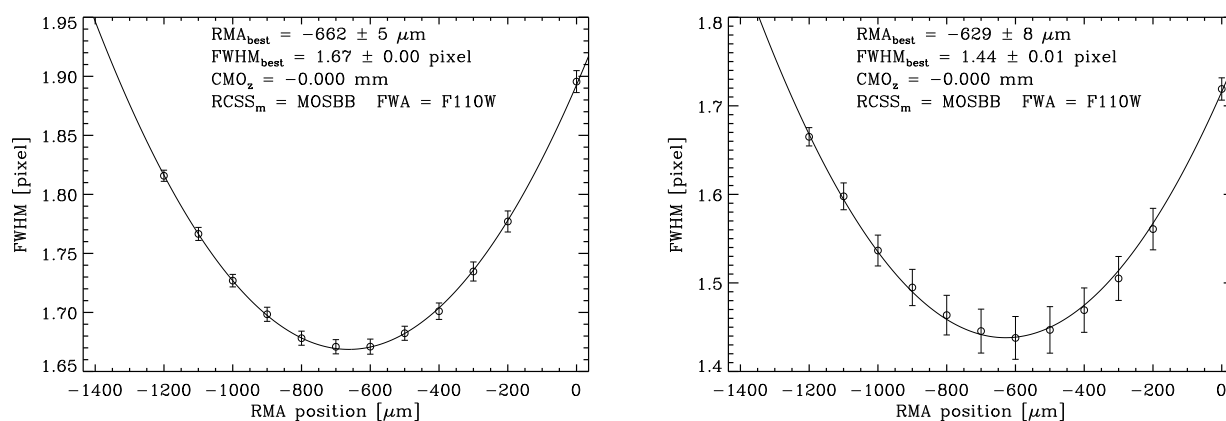

Figure 6: Focus curves for the RCSS. The data on the left was obtained using all 88 groups of the exposures, for the plot on the right only the first 22 groups were used.
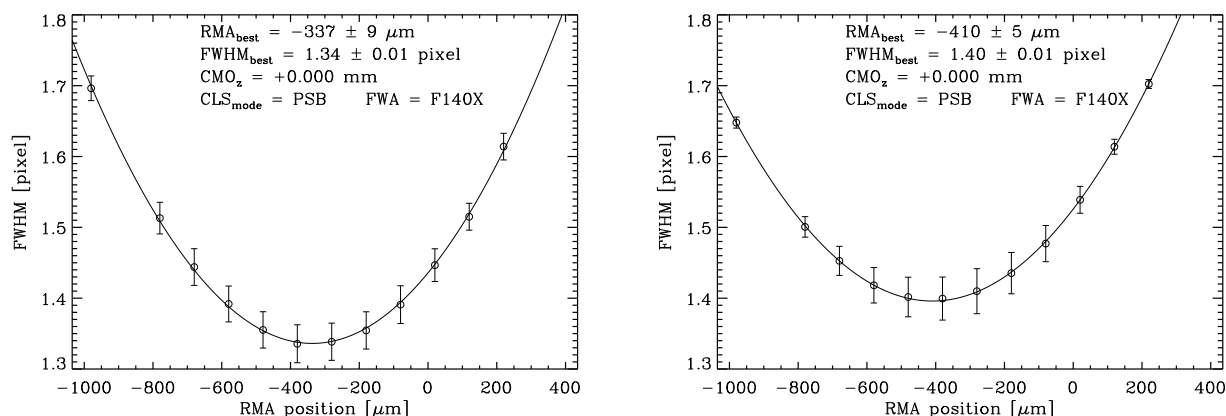
Figure 7: PHM focus curves obtained at "cold" (left) and "hot" (right) NIRSpec operational temperatures.

4.4   Confirmation phase

Towards the end of the first calibration campaign, NIRSpec was brought to its "hot" operational temperature ($T_{bench} = 43\,$K) and a subset of tests were repeated as sanity checks. A PHM focus sweep with the CMO in its nominal position was done in the test sequence `IMA-FOCUS-SHORT` and the results are shown in Fig. 7.

According to this analysis, the best focus position is slightly different (ΔRMA $\approx -70\,\mu$m) compared to the "cold" phase, and the FWHM appears marginally wider. Currently, there is no firm explanation for both effects, as NIRSpec features an athermal design and the best focus position should not change due to (small) temperature differences. The change in focus could be explained by a small displacement of the CMO that might have occurred during the course of the calibration campaign. However, this does not apply to the apparently increased size of the FWHM.

5   SUMMARY AND CONCLUSION

The analysis presented in this report indicates that NIRSpec will be capable of obtaining best focus using its RMA. All seven filters in the FWA appear to be confocal, and the best focus position for the IFU matches the one at the fixed slits to better than $100\,\mu$m (RMA translation). Thus, NIRSpec is expected to meet its focus related requirements spelled out in the FRD.

6   REFERENCES

Birkmann, S. 2011a, Description of the NIRSpec optical ground support equipment (OGSE), NIRSpec Technical Note NTN-2011-002, ESA/ESTEC

Birkmann, S. 2011b, Description of the NIRSpec pre-processing pipeline, NIRSpec Technical Note NTN-2011-004, ESA/ESTEC

Ferruit, P. 2011, Overview of the NIRSpec first cryogenic testing campaign (CYCLE1), NIRSpec Technical Note NTN-2011-001, ESA/ESTEC

Sirianni, M. & the SOT. 2011, Features and Anomalies in Cycle-1 Data, NIRSpec Technical Note NTN-2011-006, ESA/ESTEC

Smith, M. 2008, Near-Infrared Spectrograph, Functional Requirements Document JWST-RQMT-002060, Revision C, GSFC

The NIRSpec SOT. 2008, Analysis of the NIRSpec Demonstration Model Measurements at Ambient, Report ESA-JWST-RP-11883, ESA/ESTEC

A   APPLICABLE REQUIREMENTS

The focus related requirements in the NIRSpec FRD read as follows (note that these were copied from the FRD and the "shall be shall have" constructs are actually in there):

NSFR-46   NIRSpec shall be shall have the same axial focus position independent of grating and filter selection.

NSFR-59   Once NIRSpec is brought into its best alignment and whenever the OTE wave front is optimized, all NIRSpec channels shall meet their performance requirements for all modes of instrument operation without requiring further OTE adjustment.

NSFR-65   The IFU shall be shall have the same axial focus position with the other NIRSpec operational modes.

B   LIST OF EXPOSURES

Table 1 lists the focus related exposures taken during cycle 1.

Table 1: List of focus related test sequences and NIDs during cycle 1.

OBS ID	NIDs[a]	Filter	Lamp[b]	CMO_z[c]	Comment
PREP-FOCUS	4442-4460	F140X	PSB	0.0	
PREP-FOCCHK	4473-4529,7	F110W	PSB	0.0	
	4474-4530,7	F100LP	PS1	0.0	
	4475-4531,7	CLEAR	PSB	0.0	centered around $0\,\mu$m, not
	4476-4532,7	F070LP	PS1	0.0	ideal, since best focus is at
	4477-4533,7	F140X	PSB	0.0	$\approx -330\,\mu$m
	4478-4534,7	F290LP	PSB	0.0	
	4479-4535,7	F170LP	PS2	0.0	
IMA-FOCUS	4760-4778	F140X	PSB	0.0	centered around $-280\,\mu$m
	4779-4797	F140X	PSB	+2.0	centered around $+320\,\mu$m
	4798-4816	F140X	PSB	-3.1	centered around $-1080\,\mu$m
PREP-FOCUS-RCSS	4830-4845	F110W	MOSBB	0.0	32×32 array (no ref. pixels)
IMA-PSF	5820-5934	F110W	MOSBB	0.0	32×2048 array, dithered
	5935-5944	F110W	NONE	0.0	background exposures
IMA-FOCUS-SHORT	6319-6337	F140X	PSB	0.0	confirmation phase

[a] Range of NIDs used. If present, the last comma separated value denotes the step size in NIDs.
[b] Can be either CLS (PSx) or RCSS (MOSBB) source. "NONE" denotes background exposures.
[c] The z-position of the CMO in mm.